Optical in-situ characterisation of carbon nanotube growth

Post-print of a peer-reviewed article published by Inderscience Publishers.
Published article available at: http://dx.doi.org/10.1504/IJNT.2012.044826

Cite as:
Ek-Weis, J., Nerushev, O., & Campbell, E. (2012). Optical *in-situ* characterisation of carbon nanotube growth. *International journal of nanotechnology*, 9(1-2), 317.

Article published: 10/01/2012

Optical *in-situ* Characterisation of Carbon Nanotube Growth**

J. Ek-Weis,[1] O.A. Nerushev,[1] E.E.B. Campbell[1]

[1]EaStCHEM, School of Chemistry, Joseph Black Building, University of Edinburgh, West Mains Road, Edinburgh, EH9 3JJ, UK.

[*]Corresponding author; e-mail: Eleanor.Campbell@ed.ac.uk, fax: +44 131 650 6453

Keywords:
carbon nanotubes, CNTs, microheaters, in situ growth studies, Raman spectroscopy, optical characterisation, chemical vapour deposition, CVD, CNT growth, nanotechnology

Abstract

In situ optical characterisation of carbon nanotube growth is reported. The nanotubes are grown on a micro-scale heater using chemical vapour deposition (CVD). Optical emission is used to characterise the temperature of the small-scale heater prior to and during growth and to monitor any temperature changes due to the interaction of the growing nanotubes with the cold gas atmosphere. *In situ* Raman spectroscopy is used to monitor the growth of single-walled nanotubes and optical microscopy is used to monitor the real time growth of multi-walled nanotube arrays. There are similarities with normal thermal CVD growth but also significant differences due to the extremely small heated surface area and the cold surrounding environment.

Introduction

Carbon nanotubes (CNT) have sparked the interest of a large community of researchers since the early nineties. Their light, hollow, nanoscale structure combined with the relationship between atomic structure and electrical properties, along with their extreme mechanical strength and thermal conductivity has made them very promising nanomaterials for a wide range of potential applications as well as being interesting objects for probing the fundamental properties of matter at the nanoscale(Harris, 2009). Already there are many products on the market that contain CNT, predominantly as components of composite materials where the nanotubes serve to provide additional strength or conductivity. Although major advances have been made in our ability to grow, manipulate, characterize and apply CNT and many interesting individual devices based on the properties of nanotubes have been demonstrated, there are still major challenges that need to be met before the full potential of their electronic properties can be exploited within the electronics industry. Ideally, one would want to be able to grow nanotubes "to order" on a chip in order to integrate the nanotube functionality with today's Si CMOS technology or be able to grow purely semiconducting or purely metallic CNT on various substrates on demand. At present it is only practically possible to select nanotubes with specific electronic properties after growth (Arnold et al., 2006). There is therefore considerable scope for further study of CNT growth techniques to provide a greater understanding of the parameters that influence the growth and to ultimately reach the goal of selective nanotube growth. Chemical vapour deposition (CVD) is the most widely applied method for CNT synthesis due to the great flexibility and simplicity of the technique. This method typically requires the presence of a metallic nanoparticle that serves to catalytically decompose hydrocarbon precursor molecules to provide the carbon source and seeds and feeds the growth of the nanotube at temperatures typically within the range 500 – 1000 ^{o}C. There are many parameters that influence the growth and the properties of the resulting nanotubes such as the material and size of the catalyst seed particle, the gas mixture composition, temperature, pressure, presence of electric field etc.. The main approach to study the influence of growth parameters on CNT formation is to vary a particular parameter and analyse the resulting nanotubes by means of electron and scanning probe microscopy or optical spectroscopy. A disadvantage of this approach is that it is *ex situ*. This means that it cannot give information on the evolution of the nanotubes

during synthesis nor can it provide direct information on the effects of varying the gas mixture during growth or what happens during the cooling to room temperature after growth. A few methods capable of studying the growth *in situ* have been reported. Among them are optical registration of film thickness and surface pyrometry (Puretzky A A 2008, Jönsson et al., 2007), Raman spectroscopy (Kaminska et al., 2007, Li-Pook-Than et al., Dittmer et al., 2008c, Picher et al., 2009), mass spectrometry of by-product gases (Kim, 2007, Meshot et al., 2009) and electron microscopy (Yoshida et al., 2008, Sharma and Iqbal, 2004). Electron microscopy can provide detailed structural information although the growth conditions are usually not comparable to the conditions typically used for growing CNT. Optical methods of *in situ* analysis can provide dynamical information in real-time although with poorer resolution. Raman spectroscopy can provide structural information but a significant problem for *in situ* spectroscopy is the strong background of thermal emission from the heater or reactor walls. One way to minimise this background emission is to reduce the emitting surface area, which is achievable with a micro-heater technique (Dittmer et al., 2008a, Dittmer et al., 2006, Dittmer et al., 2008c, Englander et al., 2003, Sosnowchik et al., 2010). In contrast to conventional CVD, no furnace or large scale substrate heating is required in this technique. The high temperatures required for CNT synthesis are instead reached, with the system used in our laboratory, by sending an electrical current between two electrode pads connected via a narrow metal bridge which is deposited on a Si chip (Dittmer et al., 2006). The small metal bridge is resistively heated, allowing CNTs to be grown from catalysts deposited on top of the metal. The heat load of this system is very low, less than 1 Watt. The reactor chamber can be made quite small since no furnace is required. This allows the reactor to be placed under a microscope and, by using objectives with high numerical aperture and a short working distance, a good spatial resolution of the growing nanotube structures can be achieved. Another interesting advantage of the micro-heater technique is that the heated part of the chip is very localised. This technique can therefore be used to synthesise CNTs directly on chips without heating the entire substrate to the high temperatures needed for nanotube synthesis, thus allowing growth at substrate temperatures compatible with Si CMOS processing.

Usage of local micro-fabricated heaters for CVD synthesis has some features which are different compared to common CVD oven reactors. These features include: room temperature of the gas impinging on the catalyst; small dimensions of the heater in comparison with all other reactor dimensions; fast removal of gaseous by-products from the reaction zone by free convection; possibility of fast heating cycles and rapid temperature changes of the small heater; possible chemical changes of the heater body and the close surroundings (within a few microns) of the substrate.

The combination of a small reactor chamber with a microscope and a spectrometer makes it possible to use non-invasive *in situ* spectroscopy methods during CNT growth. In this study, we apply the *in situ* optical spectroscopy possibilities for measurements of the heater temperature, Raman spectroscopy of single walled CNT growth and optical observation of the growth of multiwalled nanotube bundles.

Experimental Set Up

The small reactor chamber used to carry out the growth studies is shown in Figure 1. It was placed on a microscope stage inside a micro-Raman spectrometer (inVia Renishaw, Raman spectrometer with microscope, back scattering registration; single grating monochromator; 5 excitation wavelength – 488 nm, 514 nm, 568 nm, 647 nm, 785 nm; spectral resolution 0.6-1 cm^{-1} depending on spectral range and grating). A chip with a micro-heater is placed under an optical port in the upper lid and contacted by gold coated needles which are connected to an external circuit. *In situ* studies of nanotube synthesis are possible through a sapphire window using a standard ×50 objective (full magnification of order x1000). The small chamber volume allows very rapid pump-out, making it possible to quickly change the gas environment and have accurate control over growth times. Vacuum /exhaust line and gas feed are connected via bellows which allows the whole chamber to be moved with respect to the probing laser beam and to localize light collection from different areas on and around the heater.

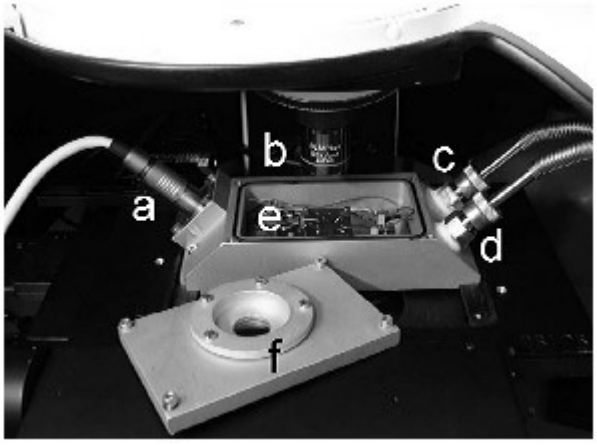

Figure 1. The chamber used for nanotube growth. (a) electrical feedthrough, (b) 15 mm long working distance objective with 50x magnification, (c) gas outlet and pump line, (d) gas inlet, (e) sample stage with contact needles, (f) upper lid with optical port.

The substrate used for the growth studies presented here is an n-type doped Si wafer with a 400 nm thick, thermally grown oxide layer. Molybdenum, with a thickness of 100 nm, is typically used as the heater material with 5 nm Ti as an adhesion layer. The heaters, with a length of 30 microns and a width of 2 microns, are patterned using electron beam lithography. A typical layout of the growth electrodes is shown in Figure 1 (b). The catalyst consists of a 1nm thick layer of Fe deposited on a 5nm thick layer of aluminium oxide. The catalyst is patterned as a series of stripes across the heater (2 microns long) with a width of 0.5 micron. The gas mixture used for multiwalled nanotube (MWNT) growth was 6 sccm (standard cubic centimetres per

second) C_2H_2, 300 sccm H_2 and 500 sccm Ar at atmospheric pressure. For growing single-walled nanotubes (SWNT), we used C_2H_4 in place of C_2H_2 . The different growth results from C_2H_2 and C_2H_4 can be related to the different carbon supply rates due to differences in dissociation activation energies (higher for C_2H_4). We have confirmed earlier the applicability of these gases for local heater growth of multi- or single-walled CNT (Dittmer et al., 2006, Dittmer et al., 2008c, Dittmer et al., 2008b). The heater was connected to an external Keithley source-meter by a 4-probe connection scheme. Four-probe connections allow higher accuracy of the heating power control and avoid errors related to the contact resistance between the contact needles and pads.

The current through the heater was controlled by a LabView program, which also measured the voltage drop across the heater. Figure2 shows a typical variation of the current and voltage during heating, exposure to the hydrocarbon gas and cooling. The example shown is for MWNT growth using acetylene as the carbon feedstock. The changes in the voltage follow the applied current (turned up step-wise) and the change of resistance of the heater. The carbon feedstock gas was introduced when the current reached its maximum value, in this case 30 mA. However, it takes approximately 25 s for the gas to flow through the gas lines and reach the heater. There is a small decrease in voltage after each increase in current which is probably related to the influence of annealing the heater material as the temperature increases. The jump in voltage after about 300 s is due to the carbonization of the heater when it is reached by the carbon feedstock gas and this leads to a further change in the resistivity of the heater. Note that this change in the heater resistance only happens during the first time it is heated and the resistance remains constant during cooling. Typical currents suitable for nanotube growth are in the range of 30-40 mA with a bias on the heater in the range of 5-10 Volts.

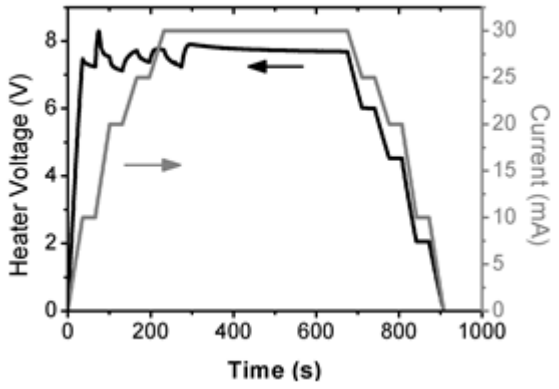

Figure 2. Typical time profile of voltage and current during MWNT growth. The current is held constant at 30 mA during growth. The voltage is seen to increase when the acetylene reaches the heater. This is attributed to carbonization of the heater material.

Temperature Measurement

Temperature is a very critical factor in the growth of CNT. The temperature of the micro-heater cannot be

determined using any contacting thermal probe since the structure is so small that any probe would itself influence the temperature (Christofferson et al., 2008). Also, the electrical resistance of the heater cannot be used to determine the temperature due to the chemical modification of the heater and corresponding resistance changes that occur during the CVD process as discussed above. The most reliable method to determine the temperature is to measure the black body emission spectrum, especially during the initial stage of growth before the nanotube coverage becomes too dense and screens the emission.

The spectrometer was calibrated using a tungsten lamp with a known emission spectrum. Spectra of emission before and after correction with the thus obtained apparatus function of the system are shown in Figure 3a. The corrected spectrum can be fitted to the Planck distribution $I(\lambda,T) \propto \lambda^{-5}(e^{hc/\lambda kT}-1)^{-1}$, where *h* is Planck's constant, *c* the speed of light, λ the emission wavelength, *k* Boltzmann's constant and *T* the temperature. By using Wien's approximation (hc >>λ kT) and rearranging the blackbody formula, it is found that $-\ln(I\lambda^5) \propto 1/\lambda T$. Consequently, the temperature can be conveniently found from the determination of the inverse gradient in a plot of $-\ln\left(I\lambda^5\right)$ versus 1/λ, see Figure 3b. The heater is not a true black-body and here we are making the additional assumption that the emissivity does not change significantly over the wavelength range of interest (grey-body assumption). The blackbody spectrum of the heater might change when its chemical composition is modified. In order to test this, blackbody spectra were recorded in different gas environments, but no changes were found. Since the emission intensity is low at short wavelengths and the detector efficiency drops rapidly at long wavelengths, only the part of the spectra (between the arrows shown in Figure 3(b)), corresponding to a wavelength range of 700 – 900 nm, is used for the temperature measurement.

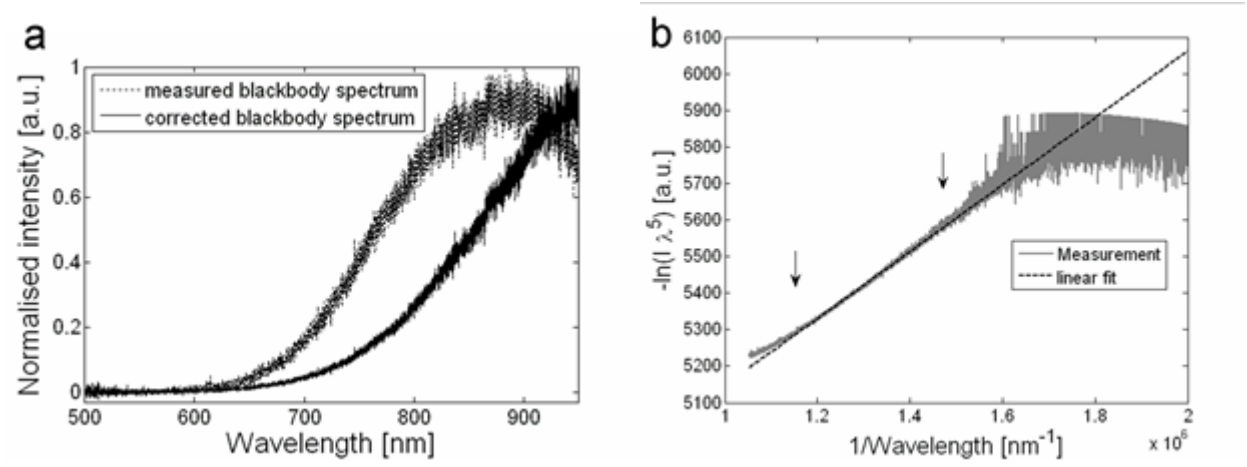

Figure 3. (a). Blackbody curves before (gray) and after (black) calibration with a tungsten lamp. (b) Corrected spectrum in Wien's coordinates showing the straight line fit used to extract the temperature.

In situ Raman Studies of SWNT Growth

The Raman spectra are masked by thermal emission from the heater and only a small fraction of the growing SWNT are resonant with the probing laser line. Raman measurements were performed only on the catalytically active surface although CNT can be found afterwards on the substrate surface extending up to 5 microns away from the heater. Figure4. depicts typical scanning electron microscope (SEM) images after SWCNT synthesis, using two different magnifications on the same substrate. The catalyst areas appear lighter than the non-coated Mo surface in these images. Individual SWNTs can be seen lying perpendicular to the heater edge on the higher magnification picture. The CNT did not grow along the substrate surface but undergo chaotic motion during growth in the convective gas flow that occurs around the hot heater. They take up the quasi-aligned arrangement on the surface after growth when the convective gas flow has ceased. This chaotic upwards motion of the CNT that occurs during growth does not allow us to perform stable reproducible *in situ* Raman measurements outside the catalytic area. We have compared two modes of "*in situ*" spectral acquisition: real time and "intermittent" mode. Real time mode refers to direct continuous spectral acquisition during a small spectral integration time but with relatively high laser power density (~0.5 $mW/\mu m^2$). The spectra that are obtained contain a significant background of thermal radiation from the heater. This limits the choice of excitation laser to short wavelengths, in our case 488nm and 514 nm lasers, where the thermal emission intensity is not very high. The main advantage of this type of acquisition is that it is a non-invasive measurement with the possibility to monitor changes in real time, but the signals are quite noisy due to the short integration times.

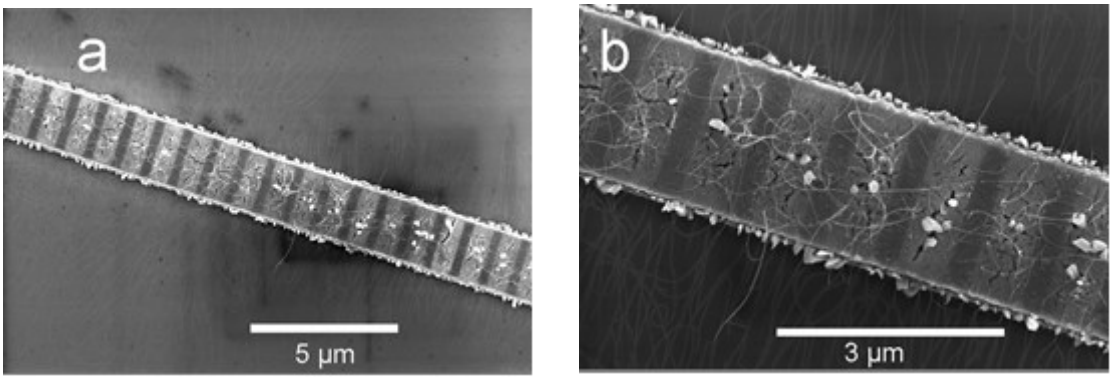

Figure4. Typical SEM images of the heater, catalyst areas and nanotubes grown using 6 sccm C_2H_4, 300 sccm H_2 and 500 sccm Ar. The brighter rectangles are areas with catalyst.

The "intermittent" mode uses the fact that the temperature of the heater can be varied very rapidly since its thermal inertia is very small. The temperature can be decreased by a few hundred degrees in less than a second. The process chamber is also small, which allows fast changes of the gas environment. The pressure in

the chamber can be reduced by two orders of magnitude in 7 seconds. The growth can therefore be stopped very quickly by decreasing the current through the heater and pumping out the carbon containing atmosphere. By stopping the synthesis at various times the growth evolution can thus be studied. This allows longer acquisition times and thereby less noisy Raman spectra to be recorded than with the real time *in situ* studies. The choice of laser excitation wavelength is not limited by thermal radiation from the surroundings in this case. However, changes in heating power, pressure and gas composition can result in significant motion of the CNTs. It is therefore not possible to follow the evolution of an individual nanotube via its radial breathing mode peak (that provides information on the nanotube diameter), instead only the statistical average can be discussed in the context of these measurements.

Optical Microscopy Observation of MWNT Growth

In contrast to SWNT growth using ethylene as carbon precursor, MWNT growth using acetylene precursor with the same type of catalyst provides growth with much higher surface density and nanotube bundles are clearly visible in an optical microscope. *In situ* real time optical detection of nanotube growth in the microscope allows the start and end times of growth to be determined with high accuracy, corresponding to the video frame frequency (ca. 0.1 second for our apparatus). Accurate *in situ* measurement of the growth rate and final length can be difficult in some cases due to the tendency of the small bundles to move in the gas flow. More accurate measurements of the length can be performed *ex situ* using SEM images recorded under different tilt angles.

Results and Discussion

In situ Raman Studies of SWNT Growth

In situ measurements of the time-development of SWNT Raman spectra were carried out for growth at a local catalyst temperature of ca. 800 °C using the procedures described above. The spectra covered the wavelength range containing the G and D bands, Figure 5a. The acquisition parameters were the same for all spectra. Under these conditions the intensity of the G band (around 1580 cm^{-1}), that corresponds to carbon-carbon vibrations parallel (G^+, at room temperature ca. 1580 cm^{-1}) and perpendicular (G^-, at room temperature ca.1540 cm^{-1}) to the nanotube axis, is proportional to the amount of SWNTs that are resonant with the excitation laser and that are within the optical probe spot. The integrated G band intensity versus time is shown in Figure5b. The intensity increases rapidly during the first minute, then slowly increases until it starts slowly decreasing after approximately 5 minutes. The nanotubes can still be growing outside of the probed region (probe diameter is approximately 1.4 micron for 514 nm excitation wavelength), but no more nanotubes are nucleated and the volume of SWNTs within the probe area is stabilised. A typical SEM image

(Figure4) shows sparsely grown SWNTs on the surface of heater.

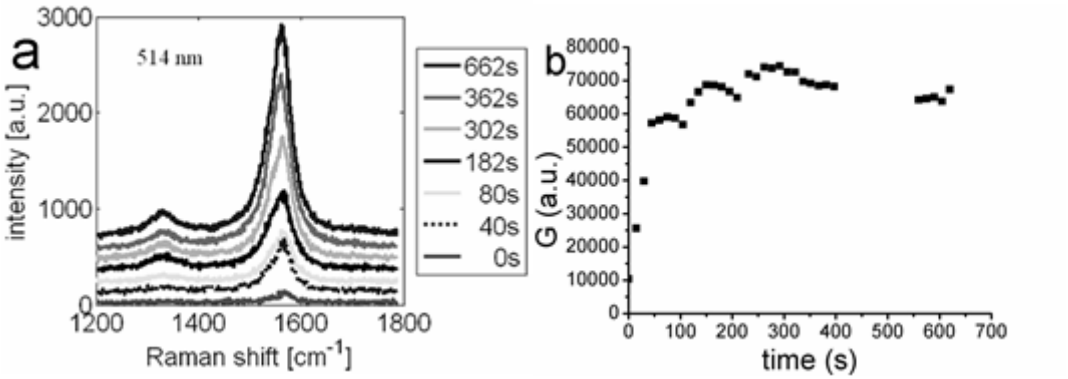

Figure 5. (a) Time series of the G, D lines region using an excitation wavelength of 514 nm. (b) Time evolution of the area of the G peak. The nanotubes were grown at 1100K using 300 sccm H_2, 500 sccm Ar and in (a) 12 sccm C_2H_4; in (b) 6 sccm C_2H_4.

The second spectral feature, at ca. 1330 cm^{-1}, is the D band which is assigned to the presence of wall defects in SWNTs and also to carbonaceous by-products with sp^3 hybridization. G/D peak ratios can be considered as a measure of the "quality" or "crystallinity" of grown nanotubes. The evolution of this ratio with time can be important for understanding the growth process. The time dependences of the development of the G/D ratios are shown in Fig 6.a-c for different ethylene flow rates for the same heater power resulting in a temperature of ca. 1100 K and with constant flow rates of other gases. A common trend for the first four gas compositions is a non-monotonic behaviour. The initial decrease of the G/D ratio in the first stage of growth is followed by a stage where there is a fast increase and after ca. 10 minutes this changes again to a slow decrease. The first drop is not very pronounced in the first plot (Fig 6a) because in the very beginning of this experiment no D line was visible above the noise level which formally can be considered as an infinite G/D ratio, these points are not plotted in the figure. This observation of a non-monotonic change in the G/D ratio differs from reported constant G/D ratios for conventional CVD reactors (Li-Pook-Than et al., Picher et al., 2009,) and may be explained by the difference in reaction environment.

The non-monotonic behaviour does not depend on the wavelength of the excitation laser. Intermittent mode measurement at the lowest flow rate was used to obtain better resolved spectra and showed a similar trend (Dittmer et al., 2008c) for four different excitation laser lines (514 nm, 468 nm, 647 nm, 785 nm). The first appearance of the D band corresponds to the presence of wall defects in the growing nanotubes and by-product amorphous carbon deposition on the heater and catalyst surfaces. The D band grows slowly since

most of the gaseous by-products that produce the amorphous carbon deposit are removed from the heater area due to the small heater width which is comparable to the molecular mean free paths. For some growth conditions, the absolute value of the D peak was even seen to decrease during the initial stage of growth. This observation can be related to annealing of amorphous carbon deposits on the surface of the heater or thermal healing of wall defects. After a few tens of seconds the growth of the G peak slows down (Figure5b) and finally stops due to full blocking of the catalyst surface by graphitic or amorphous carbon. The trend of the G/D ratio changes from growing to slowly decreasing after this. This decrease corresponds to the increase of non catalytic carbon deposition on the heater and SWNT surfaces. For the highest ethylene flow rate of 30sccm (Fig 6d), the catalyst blocking happens almost immediately after the carbon has been introduced into the system. SEM images of grown material confirm a much smaller amount of nanotubes with shorter average length in the last case. The D peak differs for the highest flow rates not only in intensity but also in spectral width. There is no clear trend in time dependence of this width and the low signal/noise ratio provides quite strong variation of this value in each experiment. For low flow rates, 6 sccm, 9sccm and 12 sccm, the D peak width variations are not significant (51±8, 66±14, 65±9 cm^{-1} correspondingly) and are consistent with D-band widths expected from the presence of amorphous carbon (Dillon et al., 2004). For 30 sccm the peak is substantially broadened 125±25 cm^{-1} indicating the additional presence of other carbon-materials such as nanocrystalline graphite (Dillon et al., 2004). The RBM spectra in Figure 7a were obtained using the "intermittent" technique where growth was stopped after 5 s, 15 s, 1 min, 5 min and 10 min growth time (Dittmer et al., 2008c). The spectral position of the RBM peaks depends on the diameter of the nanotube according to the formula $\omega_{RBM} = \alpha/d + \beta$, where ω_{RBM} is the peak position(cm^{-1}), α and β are constants and d is the diameter(nm). Several different α and β values have been reported (Brar V. W. et al., 2005). However, peaks around 120 cm^{-1} and around 200 cm^{-1} correspond to diameters of 2.1-2.2 nm and 1.2-1.3 nm respectively. It is clear from both the Raman spectra in Figure 7a and the corresponding SEM images (not shown) that small diameter SWNT grow very quickly and can be seen growing out from the electrode even after 5 s with a growth rate of at least 1 μm per second. As the growth time increases, the RBM region of the Raman spectra becomes more dense and the distribution of nanotube diameters represented by the RBM peaks broadens and, in particular, appears to shift to lower wave numbers, i.e. larger diameters. A similar trend can also be seen for the real time *in situ* studies shown in Fig 7b. The same conclusion may be drawn from analysis of the G-band structure (Fig5a). Although the double peak structure of the G band consists of overlapping signals from different nanotubes it may be fitted with 2 peaks (G^+, ca. 1570 cm^{-1} and G^-, ca.1540 cm^{-1} at the growth temperature). The observed visual narrowing of the G-band with time is the result of these peaks moving closer together. Earlier investigations of Raman spectra of individual single walled tubes (Jorio et al., 2003, Bose et al., 2005, Paillet et al., 2006) have shown that the G^- peak moves further away from the G^+ peak as the nanotube diameter decreases (due to the increasing curvature along the circumference of the tube influencing the frequency of the carbon-carbon modes that are quasi-perpendicular to the nanotube axis).

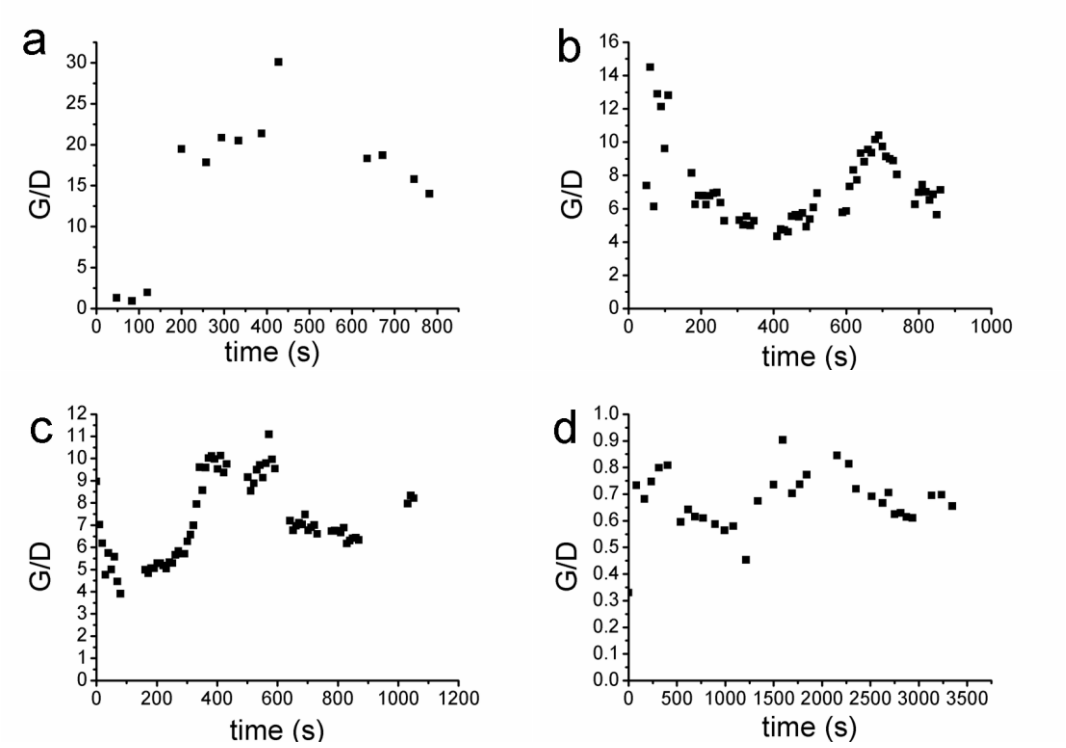

Fig 6. Time evolution of the G/D ratio for different ethylene flow rates. (a) 6 sccm; (b) 9 sccm; (c) 12 sccm; (d) 30 sccm. The growth conditions were otherwise identical, 300 sccm H_2 and 500 sccm Ar at 1100 K; excitation wavelength 514 nm.

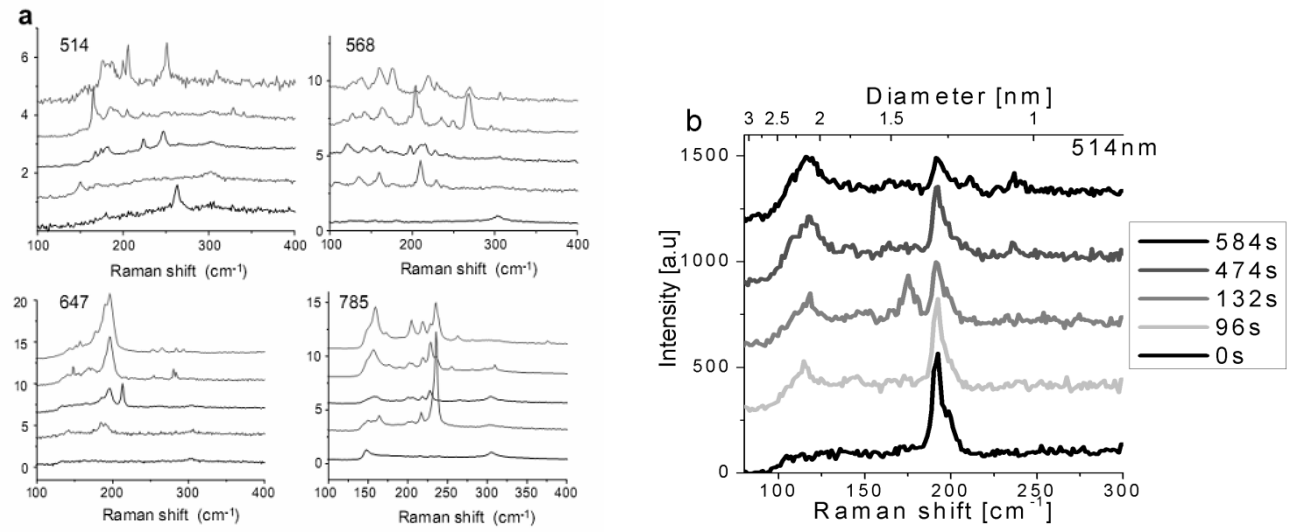

Figure 7. (a) Raman spectra in the RBM region for four different laser wavelengths obtained using the "intermittent" mode. The growth time in each plot increases from bottom to top, and was 5 s, 15 s, 1 min, 5 min and 10 min. The excitation wavelength is denoted in nanometres in each corresponding quarter. (b) Raman spectra in the RBM region obtained in real time using a laser wavelength of 514 nm.

In situ Optical Studies of MWNT Growth

MWNTs were grown on chips with the same design as was used for the SWNT growth but at a lower temperature (700-750 ^{o}C) and using C_2H_2 instead of C_2H_4 as the carbon feedstock gas. The catalyst was patterned as an array of stripes (0.5 by 2 microns, as before) with variable distances between them. The first set of experiments was performed with a small separation of the catalyst stripes (0.5 micron). For such dense packing of the catalyst it is difficult to quantify any temperature change that may occur on the heater due to the rapid screening of the heater as the thick MWNT layer grows. In addition to an increase in temperature, due to changes in the electrode material leading to an increased resistivity when the heater is exposed to the carbon feedstock, there may also be a cooling contribution from the thick nanotube bundles growing into the cold gas atmosphere. The growth of CNTs was recorded by a video camera connected to a microscope, focused on the Si surface. A set of snapshots from one of these movies is shown in Figure8a. The nanotubes form a dense film after a few seconds (Figure8a, 50 s), which grows vertically. This nanotube array continues to grow vertically until it loses its stability (Figure8a, 68 s) due to the turbulent gas flow above the heater. The amplitude of the nanotube array motion increases until the outer edge of the array reaches the surface of the chip (Figure8a, 80 – 163 s). The contact of the edge with the substrate limits the vertical motion and brings this edge into the focus of the video camera while the middle part continues to move and remains out of focus. In the final stage (Figure8a, 300 s), the optical image continues to become darker on the heater, indicating the increasing optical thickness of the nanotube coverage on top of the heater. Fig8b. shows a SEM image of the typical structure of nanotubes grown under these conditions.

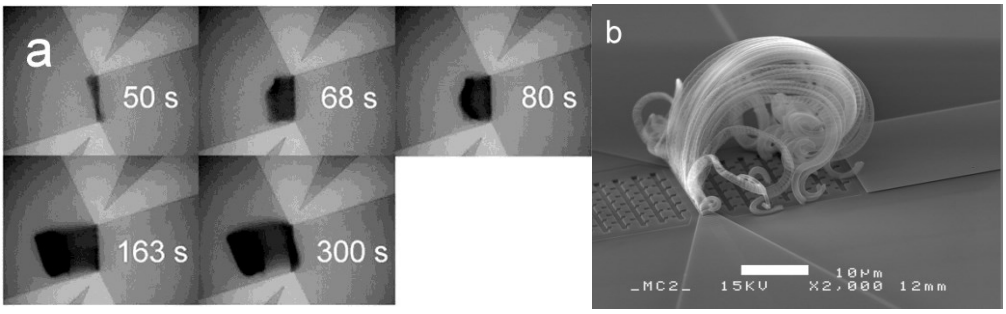

Figure 8. (a). Snapshots from MWNT growth using 6 sccm C_2H_2, 300 sccm H_2 and 500 sccm Ar. Time is counted from when the current reached its highest value and the feedstock gas was introduced, after about 4 minutes compared to Figure 2. The catalyst was deposited as small rectangles (2 µm x 0.5 µm) separated by 0.2 µm. (b) Typical SEM image of nanotubes grown under these conditions.

Further experiments with 3 small catalyst areas were done to quantify any influence of heater cooling through MWNT interaction with the cold gas. The nanotubes themselves are significantly colder than the heater surface and are not seen to emit radiation in the optical range. The position of the catalyst is clearly visible on the images shown in Figure 9.

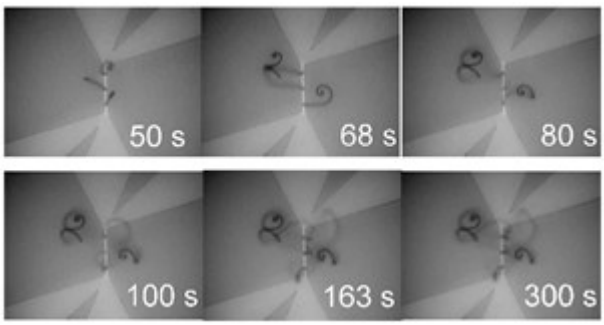

Figure 9. Snapshots from MWNTs growth using 6 sccm C_2H_2, 300 sccm H_2 and 500 sccm at 1100 K.

Time is counted from when the current reached its highest value and the feedstock gas was introduced, after about 4 minutes compared to Figure 2. The catalyst was deposited as small rectangles (2 μm x 0.5 μm) separated by 10 μm.

Temperature measurements were performed (Figure10) simultaneously with the video recording. Initially (except points marked by arrows) spectra were obtained quite close to the central catalyst stripe. The initial temperature after the heating process (explained above) was found to be 1020 K, that is after the current had reached the desired value but before the hydrocarbon had reached the heater. The introduction of C_2H_2 then increased the temperature to 1110 K, after which there is an indication that it slowly dropped. This drop can be related to annealing of the heater and its carbonization, as discussed above in connection with Figure2, where a sudden increase in the voltage across the heater can be seen when the carbon gas reaches it, followed by a slow voltage decrease. The temperature drop is however on the level of the uncertainty of the measurements. The same trend is observed when ethylene is used instead of acetylene and also for a heater without any deposited catalyst. After 5 minutes the measurement spot was moved closer to the catalyst where a temperature of 1070 K was measured. The temperature a few microns away, in the region halfway between the catalyst stripes, was found to be approximately 70 K higher. We attribute the change in temperature along the heater surface to be related to the efficient cooling of the MWNT bundles.

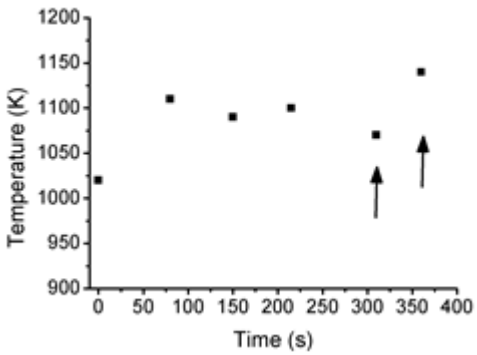

Figure 10. Heater temperature corresponding to the video frames in Figure8 and the voltage/current profile in Figure2 (with time offset ca. 4 minutes compared to Figure 2).

Visual observation does not provide quantitative information on MWNTs growth but is important for technological control and can be used for visualization of nanotube motion control by gas flow or external fields. With the present design, visual observation allows us to determine optimal growth conditions and investigate the factors leading to growth termination.

Conclusion

Optical *in situ* studies in combination with the local heater technique provide a means for determining and optimizing parameters for on-chip growth in real time experiments. This analysis can be especially helpful if electron microscopy, which is known to damage nanotubes, is to be avoided. Different growth phases can be identified by real-time video recording of dense MWNT bundle growth or by real-time Raman spectroscopy of the spectral range of G, D and RBM lines. Features in the Raman spectra allow the purity of the nanotube material to be assessed.

References

[1] ARNOLD, M. S., GREEN, A. A., HULVAT, J. F., STUPP, S. I. & HERSAM, M. C. (2006) Sorting carbon nanotubes by electronic structure using density differentiation. *Nat Nano,* 1**,** 60-65.

[2] BOSE, S. M., GAYEN, S. & BEHERA, S. N. (2005) Theory of the tangential G-band feature in the Raman spectra of metallic carbon nanotubes. *Phys. Rev. B: Condens. Matter Mater. Phys. FIELD Full Journal Title:Physical Review B: Condensed Matter and Materials Physics,* 72**,** 153402/1-153402/4.

[3] BRAR V. W. , SAMSONIDZE GE. G., SANTOS A. P. , CHOU S. G., CHATTOPADHYAY D. , KIM S. N. , PAPADIMITRAKOPOULOS F. , ZHENG M. , JAGOTA A. , ONOA G. B. , SWAN A. K. , ÜNLÜ M. S. , GOLDBERG B. B. , DRESSELHAUS G. & S., D. M. (2005) Resonance Raman Spectroscopy Characterization of Single-Wall Carbon Nanotube Separation by their Metallicity and Diameter. *Journal of Nanoscience and Nanotechnology,* 5**,** 209–228.

[4] CHRISTOFFERSON, J., MAIZE, K., EZZAHRI, Y., SHABANI, J., WANG, X. & SHAKOURI, A. (2008) Microscale and Nanoscale Thermal Characterization Techniques. *Journal of Electronic Packaging,* 130**,** 041101-6.

[5] DILLON, A. C., YUDASAKA, M. & DRESSELHAUS, M. S. (2004) Employing Raman Spectroscopy to Qualitatively Evaluate the Purity of Carbon Single-Wall Nanotube Materials *Journal of Nanoscience and Nanotechnology,* 4**,** 691-703.

[6] DITTMER, S., MUDGAL, S., NERUSHEV, O. A. & CAMPBELL, E. E. B. (2008a) Local heating method for growth of aligned carbon nanotubes at low ambient temperature. *Low Temperature Physics,* 34**,** 834-837.

[7] DITTMER, S., MUDGAL, S., NERUSHEV, O. A. & CAMPBELL, E. E. B. (2008b) Local heating method for growth of aligned carbon nanotubes at low ambient temperature. *Low Temp. Phys. FIELD Full Journal Title:Low Temperature Physics,* 34**,** 834-837.

[8] DITTMER, S., NERUSHEV, O. A. & CAMPBELL, E. E. B. (2006) Low ambient temperature CVD growth of carbon nanotubes. *Applied Physics A: Materials Science & Processing,* 84**,** 243-246.

[9] DITTMER, S., OLOFSSON, N., EK WEIS, J., NERUSHEV, O. A., GROMOV, A. V. & CAMPBELL, E. E. B. (2008c) In situ Raman studies of single-walled carbon nanotubes grown by local catalyst heating. *Chemical Physics Letters,* 457**,** 206-210.

[10] ENGLANDER, O., CHRISTENSEN, D. & LIN, L. (2003) Local synthesis of silicon nanowires and carbon nanotubes on microbridges. *Applied Physics Letters,* 82**,** 4797-4799.

[11] HARRIS, P. J. F. (2009) *Carbon Nanotube Science: Synthesis, Properties and Applications,* Cambridge,

Cambridge University Press.

[12] JÖNSSON, M., NERUSHEV, O. A. & CAMPBELL, E. E. B. (2007) In situ growth rate measurements during plasma-enhanced chemical vapour deposition of vertically aligned multiwall carbon nanotube films. *Nanotechnology,* 18**,** 305702.

[13] JORIO, A., PIMENTA, M. A., SOUZA FILHO, A. G., SAMSONIDZE, G. G., SWAN, A. K., UNLU, M. S., GOLDBERG, B. B., SAITO, R., DRESSELHAUS, G. & DRESSELHAUS, M. S. (2003) Resonance Raman Spectra of Carbon Nanotubes by Cross-Polarized Light. *Phys. Rev. Lett. FIELD Full Journal Title:Physical Review Letters,* 90**,** 107403/1-107403/4.

[14] KAMINSKA, K., LEFEBVRE, J., AUSTING, D. G. & FINNIE, P. (2007) Real-time in situ Raman imaging of carbon nanotube growth. *Nanotechnology,* 18**,** 165707.

[15] KIM, S.-M., ZHANG, Y., TEO K.B.K., BELL, M.S., GANGLOFF, L ., WANG X., MILNE W.I., WU J., JIAO, J. & LEE, S.-B. (2007) SWCNT growth on Al/Fe/Mo investigated by in situ mass spectroscopy. *Nanotechnology,* 18**,** 185709.

[16] LI-POOK-THAN, A., LEFEBVRE, J. & FINNIE, P. Phases of Carbon Nanotube Growth and Population Evolution from in Situ Raman Spectroscopy during Chemical Vapor Deposition. *The Journal of Physical Chemistry C,* 114**,** 11018-11025.

[17] MESHOT, E. R., PLATA, D. E. L., TAWFICK, S., ZHANG, Y., VERPLOEGEN, E. A. & HART, A. J. (2009) Engineering Vertically Aligned Carbon Nanotube Growth by Decoupled Thermal Treatment of Precursor and Catalyst. *ACS Nano,* 3**,** 2477-2486.

[18] PAILLET, M., MICHEL, T., MEYER, J. C., POPOV, V. N., HENRARD, L., ROTH, S. & SAUVAJOL, J. L. (2006) Raman Active Phonons of Identified Semiconducting Single-Walled Carbon Nanotubes. *Physical Review Letters,* 96**,** 257401.

[19] PICHER, M., ANGLARET, E., ARENAL, R. & JOURDAIN, V. (2009) Self-Deactivation of Single-Walled Carbon Nanotube Growth Studied by in Situ Raman Measurements. *Nano Letters,* 9**,** 542-547.

[20] PURETZKY A A , E. G., ROULEAU C M. , IVANOV I N AND GEOHEGAN D B (2008) Real-time imaging of vertically aligned carbon nanotube array growth kinetics. *Nanotechnology,* 19**,** 055605.

[21] SHARMA, R. & IQBAL, Z. (2004) In situ observations of carbon nanotube formation using environmental transmission electron microscopy. *Applied Physics Letters,* 84**,** 990-992.

[22] SOSNOWCHIK, B. D., LIN, L. & ENGLANDER, O. (2010) Localized heating induced chemical vapor deposition for one-dimensional nanostructure synthesis. *Journal of Applied Physics,* 107**,** 051101-14.

[23] YOSHIDA, H., TAKEDA, S., UCHIYAMA, T., KOHNO, H. & HOMMA, Y. (2008) Atomic-Scale In-situ Observation of Carbon Nanotube Growth from Solid State Iron Carbide Nanoparticles. *Nano Letters,* 8**,** 2082-2086.